PROCEEDINGS OF SCIENCE

Neutron Monitor Comparison by Spectral Analysis in relation to Cosmic Ray Intensity in the period 2013-2018

A. López-Comazzi[*‡]
U.Alcalá, Spain
E-mail: alejandrofrancisco.l@edu.uah.es

J.J. Blanco
U.Alcalá, Spain
E-mail: juanjo.blanco@uah.es

Morlet Wavelet Analysis is applied to the period 2013–2018 corresponding to the decreasing phase of the solar cycle 24. The aim is to identify characteristic periodicities between days to one years in the neutron monitor counting rates of a set of 22 neutron monitors distributed around the world and at different elevation above sea level (a.s.l). Six periodicities are observed once the one day period is removed: The synodic solar rotation (27–28.3 days) and its second harmonic, the near annual period and 47, 93 and 133 days periods. The last one is especially strong since 2014. An artificial neutron monitor power spectrum has been built by averaging the obtained power spectrum of the 22 neutron monitors. This average power spectrum is used as reference for the rest of neutron monitors. After the comparison, we have defined two indices, Q_j and Q_x, the first one determines how much the power spectrum of a single station differs with respect to the reference spectrum and the second one is the weighted cross-correlation between a single neutron monitor and the other 21. Finally, we define a station factor quality as the mean value of Q_j and Q_x.

36th International Cosmic Ray Conference
July 24th - August 1st 2019
Madison, Wisconsin, USA

[*]Speaker.

[†]Thanks to project CTM2016-77325-C2-1-P funded by Ministerio de Economía y Competitividad and by the European Regional Development Fund, FEDER.

[‡]Thanks to MINECO - FPI 2017 Program cofinanced by the European Social Fund.

PoS(ICRC2019)1108

1. Introduction

The primary cosmic rays (CR) are electrically charged high energy particles, mostly originating in violent phenomena of our galaxy (such as supernova explosions, pulsars with very strong magnetic fields) and, to a lesser extent, solar or extragalactic phenomena, that continuously affect the terrestrial atmosphere with energies between 10^6 and 10^{20} eV. When these primary CR interact with particles present in the Earth's atmosphere, other particles called secondary cosmic rays, such as protons, neutrons and mesons are created, these last two particles are registered by ground-based neutron monitors (NM) and Muon telescopes respectively.

The first neutron monitor with the "NM64" standard, a standard to obtain data which to compare with other stations, has been operating since 1957. From that date to the present day, other similar instruments have been developed along different positions on the terrestrial sphere. Most of them share their measurements through the Neutron Monitor Data Base (NMDB). Cosmic Rays Intensity (CRI) is anticorrelated to the solar activity with a certain delay caused by irregularities in the Interplanetary Magnetic Field [1]. The historical maximum value of the CRI measured by the neutron monitors is being registered during this year 2019, previously, the maximum value of the CRI was recorded at the end of Solar Cycle (SC) 23, at the solar minimum between 2007–2009 [2]. It was an unusual minimum followed by a weak solar maximum in the SC 24 (2012–2014) compared to the last previous cycles. It will be interesting to compare the characteristics of the modulation of CR during the current solar minimum with the previous one.

Many studies have studied the common periodicities both in the CRI and the solar parameters. Three periodicities stand out, among others, from these studies: the 27–day period, the Rieger-type period ($\sim$ 154 days) and the 11–year period, between other periodicities.

The cosmic ray flux presents quasi-periodic modulations of 27 days. This phenomenon is attributed to the solar rotation and is related to the coronal holes and co-rotating interaction regions (interactions between fast and slow solar streams) [3]. Ahluwalia compares the modulation of cosmic rays between the SC 24 and the SC 20–23 and he concludes that this modulation is significantly weaker in the SC 24 although the variation of CRI with the magnetic rigidity is similar in all the SC studied. The anomaly of the SC 24 motivates to perform spectral analysis of neutron monitors with different magnetic rigidities in order to understand the causes of the CR variations [4]. The well-known Rieger-type periodicity was firstly observed in the gamma-ray flares around the SC 21 by Rieger [5]. This periodicity was also observed by Kudela [6] in the CRI. This period is not stable and only appears around solar maximum during the polarity change.

This paper is organized the following way: In Section 2 it is described the data used and the Wavelet Analysis method; in Section 3 we present the results obtained and finally, in Section 4 the summary and the conclusions are described.

2. Data and analysis method

In the present study we use one hour pressure corrected CRI collected by the fifty-three neutron monitor stations with different values of cutoff rigidity, latitude, longitude and altitude. The stations that had less than 5% of missing values and outliers were included in this study. 26 of 53 NMs verified the condition and four of these 26 were removed because their spectra differ from the spectrum of the other monitors (this point will be explained further on Subsection 3.1). The 22 stations

and their characteristics are listed in Table 1. Dataset cover the period from January the 1^{st} 2013 to December the 31^{th} 2018 and it was downloaded from http://www.nmdb.eu/nest/, the main website of the NMDB, and http://cr0.izmiran.ru/common/links.htm. In this same period, we also applied the Wavelet Analysis to solar wind parameters such as solar wind speed, temperature, magnetic field and their components downloaded from the web https://cdaweb.sci.gsfc.nasa.gov/index.html/.

Usually other studies consider outliers or atypical values, the data outside the interval $\bar{x} \pm k\sigma_x$, being σ_x the standard deviation of the data, $\bar{x}$ the mean value and k is an integer number whose value is 1, 2 or 3 depending of the study. This outlier detection criterion is only applicable to normal distributions, then we checked if the data used in this study follow a normal distribution. For it we applied three normality tests to the flux of cosmic rays: the Kolmogorov-Smirnov test, the Jarqua-Bera test and the Anderson-Darling test. From all of them, can be concluded that the CRI in the period 2013-2018 does not follow a normal distribution. Then, we performed the analysis of Box and Whiskers, a robust method to detect outliers which only depends on the data and not on the distribution of the data. The points out of the range $[Q_1 - 1.5\,(Q_3 - Q_1)\,, Q_3 + 1.5\,(Q_3 - Q_1)]$, being Q_1 and Q_3 the first and third quartile respectively, were considered outliers. The set of outliers and missing values were corrected by linear interpolation and its percentage with respect to the total set of points for a given neutron monitor is collected in Table 1 in the variable *P.C.P* (Percentage of corrected points). The stations with $P.C.P > 5\%$ were left out of the analysis.

We applied the Wavelet Analysis to the CR Intensity to obtain the periodicities in the range 2-512 days. This method decomposes a signal into a sum of wavelets which come from a "mother" wavelet function, in this case the Morlet function [7]. The Wavelet Transform applied to a discrete sequence is

$$X(a,b) = \sum_t x(t) \cdot \Psi^*_{a,b}(t) \tag{2.1}$$

where $x(t)$ are the different points of the signal and $\Psi^*_{a,b}$ is the cojugate complex of the "mother" wavelet function and the coefficients a and b are relative to the scale and the translation of the wavelet respectively. Concretely, we used the "mother" Morlet function with $\beta = 1$, i.e

$$\Psi_{a,b}(t) = \pi^{-1/4} e^{i\omega t} e^{-t^2/2}. \tag{2.2}$$

Spectral Power P is given by the square of the Wavelet Transform which is a complex number, $P = |X(a,b)|^2$. The Wavelet Power Spectrum (WPS) shows the temporal distribution of the Spectral Power for each period and on the other hand, the Global Wavelet Spectrum (GWS) is the average of the Spectral Power at each period or resolution level. An artificial neutron monitor (Average station) power spectrum has been built by obtaining a superposed-epoch of the 22 neutron monitors. This average power spectrum is used as reference for the rest of neutron monitors.

3. Results

The Wavelet Analysis applied to the neutron monitors considered in this study presents, in general, similar results and the Figure 1 shows the WPS and GWS of two selected stations which can represent the general behaviour of the set of NMs selected in this work. The 1–day period,

ID	Station	Latitude (deg)	Longitude (deg)	Altitude (m.a.s.l)	R_C (GV)	Location (Country)	P.C.P (%)
AATB	Alma-Ata	43.04	76.94	3340	6.69	Kazakhstan	3.78
APTY	Apatity	67.57	33.39	181	0.65	Russia	0.09
ATHN	Athens	37.97	23.78	260	8.53	Greece	2.78
CALM	CaLMa	40.64	-3.16	708	6.95	Spain	4.08
HRMS	Hermanus	-34.43	19.23	26	4.44	South Africa	0.42
INVK	Inuvik	68.36	-133.72	21	0.30	Canada	2.43
JUNG	Jungfraujoch	46.55	7.98	3570	4.49	Switzerland	0.42
LMKS	Lomnicky Stit	49.20	20.22	2634	3.84	Slovakia	1.23
MRNY	Mirny	-66.55	93.02	30	0.03	Antartica	2.36
MXCO	Mexico City	19.33	-99.18	2274	8.20	Mexico	4.63
NAIN	Nain	56.55	-61.68	46	0.30	Canada	1.10
NANM	Norm-Amberd	40.37	44.25	2000	7.10	Armenia	4.06
NEWK	Newark	39.68	-75.75	50	2.40	USA	0.88
OULU	Oulu	65.05	25.47	15	0.80	Finland	0.03
PTFM	Potchefstroom	-26.68	27.09	1351	6.94	South Africa	1.35
PWNK	Peawanuck	54.98	-85.44	53	0.30	Canada	4.56
ROME	Rome	41.86	12.47	0	6.27	Italy	0.90
SOPB	South Pole 12-Bares	-90.00	0.00	2823	0.10	South Pole	0.19
SOPO	South Pole	-90.00	0.00	2820	0.10	South Pole	0.42
TERA	Terra Adelie	-66.65	140.00	32	0.01	Antartica	2.10
THUL	Thule	76.50	-68.70	26	0.30	Greenland	0.11
YKTK	Yakutsk	62.01	129.43	105	1.65	Russia	1.75

Table 1: Features of the different NM used in this work. R_C is the magnetic rigidity and P.C.P is the Percentage of Corrected Points by linear interpolation.

associated with the terrestrial rotation, was observed in all stations but it has not been included in this study because we are only interested in extraterrestrial phenomena.

All stations present similar behaviour. As a way of example, we showed the analysis for JUNG and HRMS. The spectrograms for JUNG and HRMS stations are presented in the upper panel of Figure 1. The time dependence of periodicities shows the near-annual signal disappearing after 2016 in JUNG although it remains visible in HRMS. The 27–day is the most prominent period and it appears throughout the entire interval except from mid-2013 to mid-2014 (the solar maximum). In general, in all stations this period was detected in the band 27–28.3 days related to the synodic solar rotation and its second harmonic (13.5 day) while the third harmonic (9 day) was observed in some NM. The $\sim$ 133–day period was identified between 2014-2016 in all NM with similar Spectral Power in the interval between 110 and 140 days. For example, Tsichla [8] and earlier studies of Joshi [9] detected the period of 133 days in solar activity. In the band 296–330 day it was obtained a significant peak with similar power in most of the stations; this peak is considered the near-annual period. Other peaks were observed in the range 45.5–51.5 days and in the band

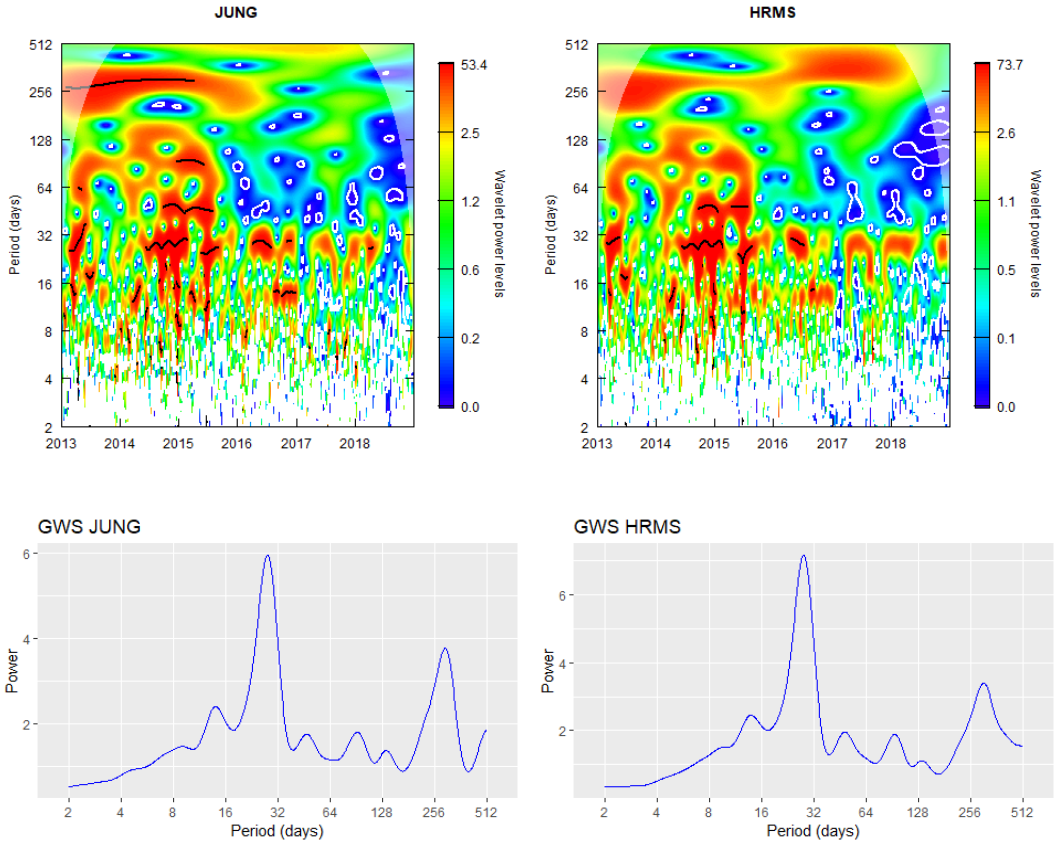

Figure 1: The WPS (up) and the GWS (down) for the Jungfraujoch (JUNG) and Hermanus (HRMS) neutron monitors.

90-95 days in the CRI. All the founded periodicities are also observed in different solar wind parameters, including these 47 and 93 periods. The Rieger period (154–day) was not detected in this study because it only occurs around the solar maximum and the latter has been very weak and Saad Farid [10] only detected it in 2012 and this year was not included in this work.

In the bottom panel in Figure 1, it is appreciated the most prominent peak of 27–day and its second harmonic (13.5–day). The second most relevant peak is the near-annual period and other three peaks can be appreciated around 47, 93 and 133 days.

3.1 Quality index based on GWS comparison

We have defined a quality factor Q_j to evaluate how much a single power spectrum differs from the one that is obtained for the reference station. The proposed quality index of each neutron monitor j is given by the following equation

$$Q_j = 1 - \frac{1}{n}\sum_{i=1}^{n}(s_{ij} - \hat{s}_i)^2 \tag{3.1}$$

where the second term is the mean squared error: s_{ij} are the points of the Global Wavelet Spectrum (GWS) obtained for a certain neutron monitor j and $\hat{s}_i$ are the points of the average GWS calculated

with all neutron monitors. This index is not normalized but if $Q_j \to 1$ implies that the station j behaves like the reference station. We consider the following criterion: if $Q_j < 0.5$ the behaviour of the station is very different from the average, if $Q_j \in [0.5, 0.65)$ the spectrum for this station is reasonable with respect to the average, for $Q_j \in [0.65, 0.85)$ the spectrum is good and finally if $Q_j \in [0.85, 1]$ is excellent. Figure 2 (a) shows the best and the worst station according to the Q_j index. Red line is the average station, blue one represents NEWK ($Q_{j=NEWK} = 0.975$) and green line is YKTK ($Q_{j=YKTK} = 0.563$).

The stations with $Q_j < 0.5$ have also been excluded from the study. These stations are not taken into account to realize the Average Spectrum and they are specifically: FSMT, JUNG1, MWSN and TXBY. Figure 2 (b) shows the GWS of the Average Station obtained with 22 NMs with $Q_j > 0.5$ (red line) and the GWS of two NM with $Q_j < 0.5$: JUNG1 (blue line) and TXBY (green line). In Table 2, the values of the quality index based on GWS comparison (with $Q_j > 0.5$) for each NM are collected.

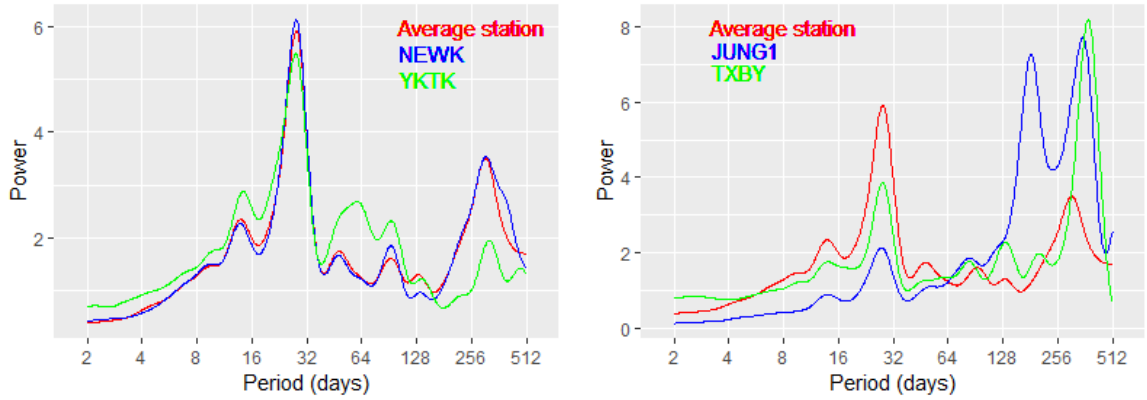

(a) (b)

Figure 2: (a) The GWS of the average station, Newark and Yakutsk. (b) The GWS of the average station, Jungfraujoch-1 and Tixie Bay.

3.2 Quality index based on cross-correlation

A second index Q_x is defined to evaluate the degree of correlation between stations:

$$Q_x = \frac{1}{N-1} \sum_{y=1, y \neq x}^{N} \max\left(\hat{\rho}_{xy}(h)\right) \tag{3.2}$$

being N the number of NM used in this study. Where

$$\hat{\rho}_{xy}(h) = \frac{\hat{\gamma}_{xy}(h)}{\sqrt{\hat{\gamma}_x(0)\,\hat{\gamma}_y(0)}}, \tag{3.3}$$

is the sample cross-correlation function between two time series x and y, and

$$\hat{\gamma}_{xy}(h) = \frac{1}{n} \sum_{t=1}^{n-h} (x_{t+h} - \bar{x})(y_t - \bar{y}), \tag{3.4}$$

Ranking	Station	Q	Q_j	Q_x	Ranking	Station	Q	Q_j	Q_x
1	NEWK	0.9506	0.9750	0.9262	12	APTY	0.9077	0.8934	0.9219
2	TERA	0.9442	0.9657	0.9227	13	PTFM	0.8929	0.8958	0.8900
3	OULU	0.9435	0.9588	0.9282	14	MXCO	0.8889	0.8717	0.9061
4	ROME	0.9315	0.9698	0.8933	15	PWNK	0.8818	0.8517	0.9120
5	JUNG	0.9270	0.9294	0.9246	16	CALM	0.8458	0.8567	0.8350
6	HRMS	0.9257	0.9188	0.9327	17	THUL	0.7858	0.6789	0.8927
7	SOPO	0.9194	0.9154	0.9234	18	AATB	0.7791	0.7495	0.8087
8	MRNY	0.9194	0.9259	0.9128	19	SOPB	0.7788	0.6399	0.9177
9	INVK	0.9121	0.8993	0.9249	20	YKTK	0.7323	0.5626	0.9020
10	NAIN	0.9102	0.9022	0.9183	21	NANM	0.7300	0.6444	0.8156
11	LMKS	0.9088	0.9022	0.9155	22	ATHN	0.7187	0.8283	0.6092

Table 2: Neutron Monitors ranking according to the quality index Q obtained by the average of the index Q_j and the index of average cross-correlation Q_x.

being n the number of points. For a station x and another station y we obtain, for each h, a value given by $-1 \leq \hat{\rho}_{xy}(h) \leq 1$. The values x_t and y_t are the CRI of the stations x and y respectively; $\bar{x}$ and $\bar{y}$ is the average value of each time series and h is the delay or temporary advance ($h = 0, \pm 1, .., \pm 20$).

As the parameter Q_j is applied to the GWS while Q_x is applied to the counting rate and these indices give slightly different results, we proposed the average indices as the final quality index:

$$Q = \frac{Q_j + Q_x}{2}, \tag{3.5}$$

where Q_j indicates the degree of similarity of the GWS of a NM with respect to the average GWS and Q_x indicates the average of the degree of correlation of a NM with the others. This index Q takes into account two things: how much the spectrum of a station differs with respect to the average spectrum and the cross-correlation between a neutron monitor with the rest.

4. Conclusions

The Morlet Wavelet Analysis is applied to the CRI of a set of 22 NM in the period 2013–2018. To detect outliers, we performed the analysis of Box and Whiskers, a robust method which only depends on the data and not on the distribution of the data. The set of outliers and missing values were corrected by linear interpolation. All the stations show similar behaviour and in their spectrum is appreciated the most prominent peak of 27–day and its second harmonic (13.5–day), the near-annual period and other three peaks can be appreciated around 47, 93 and 133 days. We have defined two indices, Q_j and Q_x, the first one determines how much the power spectrum of a single station differs with respect to the average spectrum and the second one is the weighted cross-correlation between a single neutron monitor and the other 21. Finally, since the indices are applied to different things (one to the GWS and other to the CRI), we defined the average indices as

final quality index Q. Table 2 shows the different stations ordered according to the average quality index Q.

Acknowledgements

Data of neutron monitors has been downloaded from NMDB page: http://www.nmdb.eu/nest/. Athens neutron monitor data were kindly provided by the Physics Department of the National and Kapodistrian University of Athens. The neutron monitor data from Inuvik, Norm-Amberd, Newark, Peawanuck and Thule are provided by the University of Delaware Department of Physics and Astronomy and the Bartol Research Institute. The neutron monitor data from the South Pole Bares and South Pole are provided by the University of Wisconsin, River Falls. The neutron monitor data from Oulu are provided by Sodankyla Geophysical Observatory. Terra Adelie neutron monitor data were kindly provided by Observatoire de Paris and the French polar institute (IPEV), France. Mexico City neutron monitor data were kindly provided by the Cosmic Ray Group, Geophysical Institute, National Autonomous University of Mexico (UNAM), Mexico. Rome neutron monitor (SVIRCO NM) is supported by INAF/IAPS-UNIRoma3 COLLABORATION. Almaty Neutron Monitor data were kindly provided by the Institute of Ionosphere, Kazakhstan Potchefstroom and Hermanus Neutron Monitor data were kindly provided by the North-West University of South Africa. Jungfraujoch neutron monitor data were kindly provided by the Physikalisches Institut, University of Bern, Switzerland. Mirny Neutron Monitor data were kindly provided by Pushkov Institute of Terrestrial Magnetism, Ionosphere and radio wave propagation (IZMIRAN) of Russian Academy of Science. Apatity Neutron Monitor data were kindly provided by Polar Geophysical Institute Russian Academy of Sciences. Tixie-Bay and Yakutsk neutron monitor data were kindly provided by the Institute OF COSMOPHYSICAL RESEARCH AND AERONOIMY of Russian Academy of Science. CaLMa neutron monitor data were kindly provided by the Space Research Group (SRG-UAH), University of Alcala, Spain. This work has been supported by the project CTM2016-77325-C2-1-P funded by Ministerio de Economía y Competitividad and by the European Regional Development Fund, FEDER.

References

[1] Munendra Singh, Y Singh, and Badruddin . Solar modulation of galactic cosmic rays during the last five solar cycles. *Journal of Atmospheric and Solar-terrestrial Physics - J ATMOS SOL-TERR PHYS*, 70:169–183, 01 2008.

[2] Harjit Ahluwalia. Sunspot activity and cosmic ray modulation at 1 a.u. for 1900–2013. *Advances in Space Research*, 54:1704, 10 2014.

[3] Peter Grieder. Cosmic rays at earth. *Cosmic Rays at Earth by P.K.F. Grieder. Elsevier Science, 2001.*, -1, 01 2001.

[4] Harjit Ahluwalia and Roger Ygbuhay. Cosmic ray 11-year modulation for sunspot cycle 24. *Solar Physics*, 290, 02 2015.

[5] E Rieger, Gottfried Kanbach, C Reppin, G H. Share, D J. Forrest, and E L. Chupp. A 154-day periodicity in the occurrence of hard solar flares? *Nature*, 312, 01 1985.

[6] K Kudela, Ján Rybák, A Antalová, and M Storini. Time evolution of low-frequency periodicities in cosmic ray intensity. *Solar Physics*, 205:165–175, 01 2002.

[7] C G. Torrence and G.P. Compo. A practical guide to wavelet analysis. *Bulletin of the American Meteorological Society*, 79:61–78, 01 1998.

[8] M. Tsichla, M. Gerontidou, and H. Mavromichalaki. Spectral Analysis of Solar and Geomagnetic Parameters in Relation to Cosmic-ray Intensity for the Time Period 1965 - 2018. , 294:15, January 2019.

[9] Bhuwan Joshi, Pramila Pant, and Poongodi Manoharan. Periodicities in sunspot activity during solar cycle 23. *Astronomy and Astrophysics*, 452, 11 2009.

[10] A.I. Saad Farid. High frequency spectral features of galactic cosmic rays at different rigidities during the ascending and maximum phases of the solar cycle 24. *Astrophysics and Space Science*, 364, 04 2019.